J Mater Sci (2008) 43:5712–5719
DOI 10.1007/s10853-008-2901-x

Structural transitions during aluminum leaching of $NiAl_3$ phase in a Raney Ni–Al alloy

Rong Wang · Houwen Chen · Zhilong Lu · Shaohong Qiu · Tsun Ko

Received: 23 October 2007 / Accepted: 22 July 2008 / Published online: 13 August 2008

Abstract Structural transitions during aluminum leaching of the $NiAl_3$ phase in a Raney nickel–aluminum alloy have been investigated by X-ray diffraction, transmission electron microscopy, high-resolution transmission electron microscopy, and X-ray energy dispersive spectroscopy. We observed that $NiAl_3$ grains cracked into crystalline nanofragments at the initial stage of leaching. A possible mechanism for the grain fragmentation was proposed based on the crystal structure of $NiAl_3$. We discovered that fcc nickel, the known active phase, coexisted with another active nickel phase with an orthorhombic structure in the Raney-Ni catalyst. The orthorhombic nickel phase was generated directly from its source phase, $NiAl_3$, and further transformed to the fcc nickel phase during aluminum leaching

Introduction

Raney-Ni is a solid catalyst developed in 1926 by Murray Raney [1, 2] and has been used extensively in liquid-phase hydrogenation reactions [3–5]. $NiAl_3$ and Ni_2Al_3 are known to be the main phases in starting alloys for preparing the catalyst, Ni–50wt%Al and Ni–50wt%Al doped with Cr, Fe, and other elements [6, 7]. Raney-Ni catalysts are produced by alkaline leaching of aluminum from starting Ni–Al alloys [4, 8, 9]. The leaching process leads to a sponge-like structure composed of nickel crystallites with a size of 5–10 nm [10–17].

Studies on leaching behaviors of Ni–Al compounds showed that leachability increases from Ni_2Al_3, $NiAl_3$ to $Al/NiAl_3$ eutectic [6, 18–20]. With respect to structural transitions during leaching, previous studies have mostly focused on the Ni_2Al_3 phase [10–13]. Knowledge on transitions of another source phase, $NiAl_3$, however, is very limited. The difficulties rest with the grain fragmentation of $NiAl_3$ during leaching [17]. More specifically, the composite electron diffraction patterns obtained hardly reveal any structural relations between the leaching product and its source phase, $NiAl_3$.

In this article, the Pearson nomenclature [21] is used for describing the structures present in the system. For instance, the symbol of oP16-$NiAl_3$ expresses a primitive orthorhombic structure with 16 atoms per unit cell, the chemical formula of which is $NiAl_3$. As a line (i.e., stoichiometric) compound, the composition of the $NiAl_3$ phase agrees exactly with its formula [22].

Colin et al. [15] proposed that aluminum leaching of the $NiAl_3$ phase first occurred along [001] direction and propagated along (020) planes (in the coordinate system that they used). Bakker et al. [14] observed that during leaching the nickel residue produced from $NiAl_3$ tended to disintegrate, while that from Ni_2Al_3 remained attached to the substrate material.

The present work investigated the structural transition, at an atomic scale, during aluminum leaching of the $NiAl_3$ phase in a Ni–50wt%Al alloy using X-ray diffraction, transmission electron microscopy (TEM), high-resolution transmission electron microscopy (HRTEM) examinations and X-ray energy dispersive spectroscopic (EDS) analyses. A grain fragmentation of $NiAl_3$ at the initial stage of leaching was observed. A new nickel phase with an

R. Wang (✉) · H. Chen · Z. Lu · S. Qiu · T. Ko
Department of Materials Physics and Chemistry, University of Science and Technology Beijing, Beijing 100083, People's Republic of China
e-mail: teacher_wangrong@sohu.com

orthorhombic structure, oP16-Ni, was discovered in the Raney-Ni catalyst.

Experiments and methods

A commercial Raney alloy powder (80–110 μm) was chosen for the study. The alloy composition is about 48.7wt%Ni–49.5wt%Al–1.0wt%Fe–0.80wt%Cr. The alloy powder was finely ground in an agate mortar and treated in a 20% sodium hydroxide solution at 30 and 50 °C each for 20 and 60 min and at 70 °C for 20, 60, and 90 min. The powder after leaching was then washed with de-ionized water and ethanol and stored in ethanol to prevent the powder from oxidation.

The structures of the powder before and after leaching were identified by X-ray diffraction with Cu Kα radiation at room temperature. The specimens for TEM and HRTEM examinations were prepared by dispersing a powder in ethanol ultrasonically and collecting it onto holey carbon-coated grids. TEM and HRTEM examinations were carried out at 200 kV in a JEM-2010 high-resolution electron microscope fitted with a Gatan 794 MultiScan CCD camera, a Gatan 622 TV rate image intensifier, and a super-thin-window INCA system for EDS analysis.

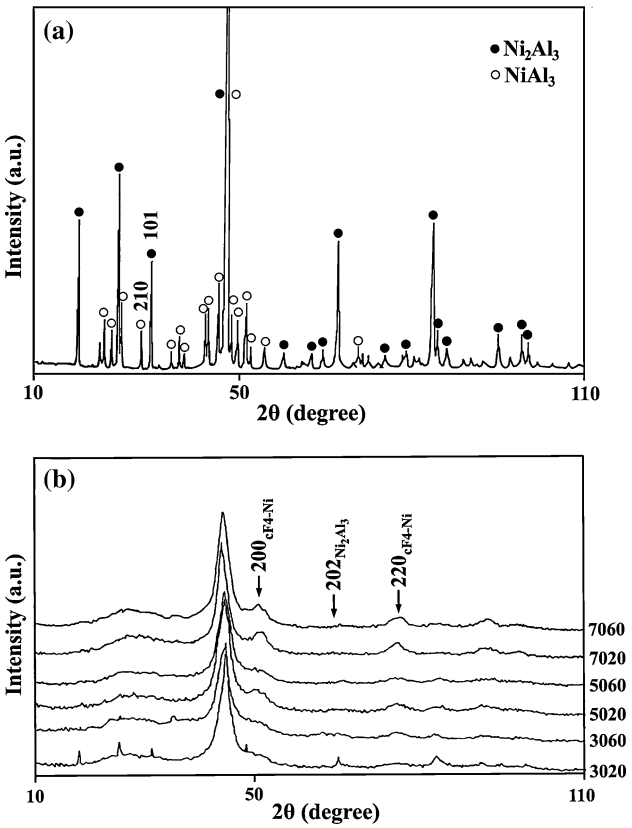

Fig. 1 X-ray diffraction spectra of (**a**) the Ni–Al alloy powder, (**b**) the Raney catalyst prepared by leaching at different conditions

Results

X-ray diffraction spectra of the Ni–Al alloy before and after leaching are shown in Fig. 1. Before leaching (Fig. 1a), the peaks on the spectrum are associated with Ni_2Al_3, $NiAl_3$, or both phases. After leaching, the background of the spectra (Fig. 1b) increases and the peaks of the $NiAl_3$ phase all merge into the background even at a low leaching temperature (30 °C) for a short leaching time (20 min). Furthermore, diffused peaks of the leaching product, cF4-Ni, emerge gradually, and their intensities increase with leaching temperature and/or leaching time.

TEM/EDS analyses revealed that the average composition (at%) of the $NiAl_3$ phase before leaching was 25.9Ni–72.8Al–0.8Fe–0.6Cr and its grain size was about 1 μm. Sponge-like agglomerates were frequently observed in the specimens after leaching under various conditions. A TEM/EDS result after leaching at 30 °C for 20 min is shown in Fig. 2. The sponge-like morphology is clearly seen on the TEM micrograph (Fig. 2a). The corresponding electron diffraction pattern and EDS spectrum are shown separately in Fig. 2b and c. The indexing result of the diffraction pattern is shown in Table 1 and arranged in the same order as those marked on the pattern. In comparison, the X-ray diffraction data for $NiAl_3$ [23] and cF4-Ni [22] are shown in the right two columns of Table 1. It is verified that all of the reflections appearing on the pattern belonged to either $NiAl_3$ or cF4-Ni, or both phases. The EDS analyses, however, showed that aluminum atoms were mostly eroded out from $NiAl_3$ and Ni_2Al_3 after leaching at 30 °C for 20 min, and that oxygen was always detected in spongy agglomerate. The composition (at%) of the spongy agglomerate shown in Fig. 2a is 58.7Ni–14.3Al–1.5Cr–25.5O. After deducting the content of oxygen, the aluminum concentration is about 19.2 at%. Together, these experimental results indicate that grain fragmentation of the $NiAl_3$ phase and aluminum leaching takes place rapidly and simultaneously at the initial stage of leaching in the present study.

A HRTEM/EDS result of the specimen after leaching at 70 °C for 90 min is shown in Fig. 3. As shown on the HRTEM image (Fig. 3a), the spongy agglomerate consists of a large amount of crystallites in the size of 3–10 nm. The diffractograms and the Fourier-filtered images of the four crystal regions framed in Fig. 3a are shown in Fig. 3b and f, c and g, d and h, e and i. Based on the measurements of the diffractograms, all four crystalline regions belong to the $NiAl_3$ structure, and their zone axes are in turn $[\bar{7}\bar{1}3]$, $[\bar{3}29]$, $[4\bar{5}2]$, and $[3\bar{5}1]$. For the angle included between the planes marked in each diffractogram, the measured value

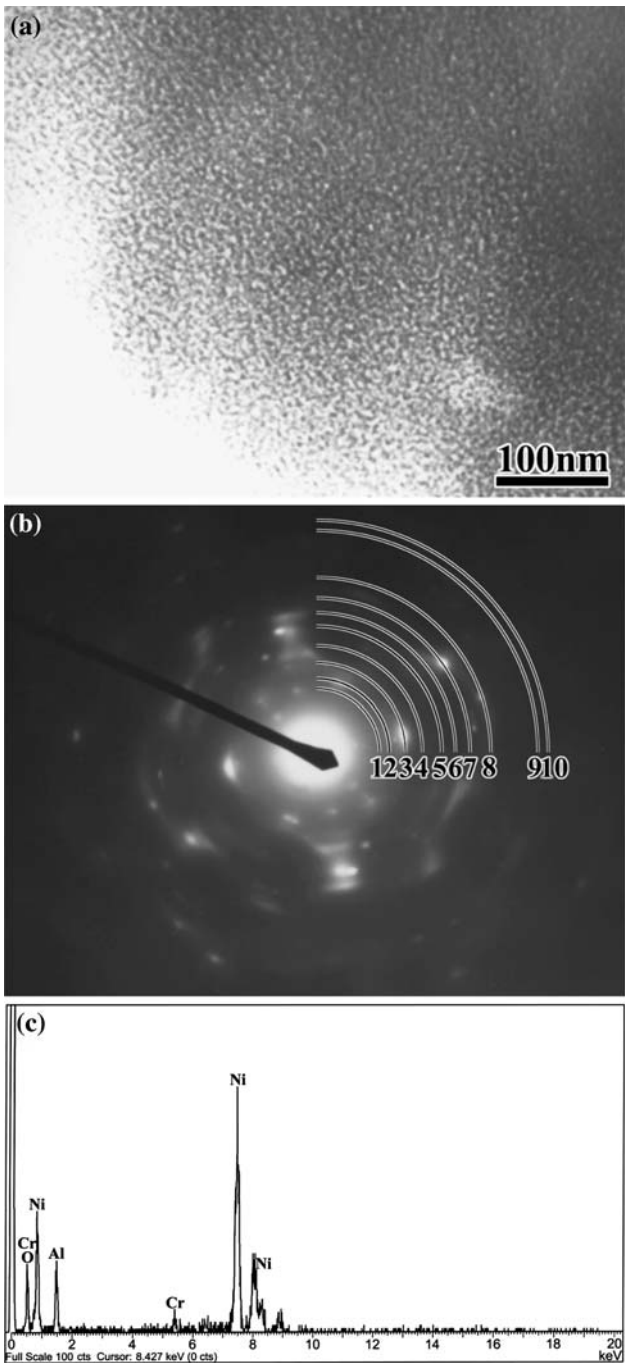

Fig. 2 (**a**) TEM image of the spongy agglomerate in the catalyst prepared by leaching at 30 °C for 20 min with (**b**) corresponding electron diffraction patterns and (**c**) EDS spectrum

all conforms to the calculated one based on the $NiAl_3$ lattice, whose values are 98° and 98.5° in Fig. 3b, 57° and 57.1° in Fig. 3c, 102° and 101.6° in Fig. 3d, and 83° and 83.0° in Fig. 3e. The EDS spectra taken from these regions were similar, and one of them is shown in Fig. 3j. The probe size chosen for EDS analyses was about 10 nm. After deducting oxygen, the aluminum concentration measured is in a range of 14–18 at%. Together with the results shown in Fig. 2, it is concluded that during leaching of the $NiAl_3$ phase at the conditions used in the study the spongy agglomerate generated consists of cF4-Ni and another type of nickel crystallites with a structure of oP16-Ni, similar to oP16-$NiAl_3$. The grain size of both cF4-Ni and oP16-Ni crystallites is at a nano-scale level. As shown in our earlier work [17], leaching at 70 °C for 90 min in a 20 wt% sodium hydroxide solution resulted in the highest hydrogenation activity for m-nitrotoluene at the reaction pressure 2.0 MPa. We propose that the oP16-Ni phase could serve as another important active phase in Raney-Ni catalyst.

Additionally, we observed that an oP16-Ni crystallite is often located adjacent to a cF4-Ni crystallite in agglomerates. An example is shown in Fig. 4. Figure 4a is a HRTEM image obtained from the specimen after leaching at 30 °C for 20 min. As indicated by the diffractogram (Fig. 4b) of the area including the "A" and "B" crystalline regions marked in the image, the region "A" belongs to the cF4-Ni phase oriented at one of $\langle 011 \rangle$ directions and the adjacent region "B" the oP16-Ni phase oriented at one of $\langle 329 \rangle$ directions, for instance the $[3\bar{2}9]$ direction with the $(30\bar{1})$ plane of oP16-Ni parallel to one of {111} planes of cF4-Ni. A semicoherent boundary was observed between the regions "A" and "B" and the illustration of the lattice image around the boundary is given in Fig. 4c. Some single-atomic steps and boundary dislocations appear clearly on the oP16-Ni/cF4-Ni boundary.

A large amount of pores existed in the spongy agglomerates of the Raney-Ni catalyst. On all HRTEM images (e.g., Figs. 3 and 4) of the spongy agglomerates, the areas with high brightness were always poorly crystallized. A high brightness on a HRTEM image implies low mass density in the corresponding area. Such a microporous region is called the boundary region (BR) in this study. BR with a size of 2–10 nm surrounds the nano-scale crystallites of the active phases. Moreover, as marked by the white broken lines in Fig. 4a, the facets of oP16-Ni and cF4-Ni nano-particles situate on the wall of the micropores, which correspond to the close packed planes of these two structures, for instance, {301} and {230} of oP16-Ni and {111} planes of cF4-Ni.

Discussion

Two important results are obtained in this study. First, we observed that grain fragmentation of $NiAl_3$ took place rapidly at the initial stage of leaching. Second, a new active phase, oP16-Ni, was discovered to coexist with the cF4-Ni phase in the Raney-Ni catalyst prepared by leaching at

Table 1 Indexing of the electron diffraction pattern shown in Fig. 2b and the X-ray diffraction data for $NiAl_3$ and the fcc nickel phases [24, 25]

Experimental			oP16-$NiAl_3$			cF4-Ni (fcc)	
Peak	Interplanar spacing d (nm)	hkl	Interplanar spacing d (nm)	Intensity	hkl	Interplanar spacing d (nm)	Intensity
1	0.39 ± 0.02[a]	101	0.389	70			
2	0.34 ± 0.01[a]	111	0.344	100			
3	0.30 ± 0.01[a]	210	0.301	60			
4	0.25 ± 0.01[a]	220	0.246	40			
5	0.201 ± 0.006[a]	131	0.207	100	111	0.203	100
		022	0.201	40			
		301	0.200	90			
6	0.178 ± 0.005[a]	321	0.176	20	200	0.176	42
7	0.167 ± 0.004[a]	400	0.165				
8	0.150 ± 0.003[a]	420	0.150				
9	0.125 ± 0.002[a]	440	0.123		220	0.124	21
10	0.108 ± 0.002[a]				311	0.106	

[a] Systematic errors based upon the precision of length measurement. The errors were calculated according to the formula $\Delta d \approx 2\frac{\Delta R}{R}d$, and the length measurement precision ΔR is estimated at 0.2 mm

30–70 °C for 20–90 min in a 20 wt% sodium hydroxide solution.

The mechanism for grain fragmentation of $NiAl_3$ during leaching

Based on the structure of $NiAl_3$ [23], we propose a possible mechanism for grain fragmentation during leaching. The structural projections of $NiAl_3$ along [010], [001], and [100] axes are presented in Fig. 5a–c, respectively. In Fig. 5a, nickel atoms are situated on the column edges of two types of hexagonal prisms, marked as ABCDEF and EFGHIJ, and aluminum atoms inside the prisms. The leaching process initiates usually from an aluminum-rich area [15] and generates passages for OH^- ions in the leaching solution. The shortest crosswise width of the passages formed by removing aluminum atoms from the prisms is about 0.23 nm (i.e., that on the line linking C and F in Fig. 5d). Notably, the atoms marked by C and F are not on a same (010) plane, the actual width of the interstice between these two atoms is about 0.34 nm.

On the other hand, as shown in Fig. 5b, c, nickel atoms are all distributed on the (020) planes. The shortest three distances between two atoms which situate on the neighboring (020) planes are in turn 0.410, 0.452, and 0.466 nm. Therefore, two types of passages can be formed simultaneously during leaching of $NiAl_3$, the prism passages along the [010] direction and the plane passages parallel to the (010) plane. This leaching process facilitates, naturally, cracking of $NiAl_3$ grains.

oP16-Ni phase and formation of spongy agglomerates in Raney-Ni catalyst

As discovered in this study, during aluminum leaching oP16-Ni is generated from the oP16-$NiAl_3$ phase. The oP16-Ni phase preserves the structure type of its source phase. Similarly, we revealed recently that the structure of oP16-$NiAl_3$ was maintained in a film specimen prepared by 3–7 keV Ar^+ ion etching of a Ni–50wt%Al alloy, even if the compound became almost a Ni phase (about 8.5–10 at% Al) [24]. Together, our results suggest that during some drastic treatments, such as ion etching and alkaline leaching, the structure of oP16-$NiAl_3$ tends to be undisturbed.

The EDS results showed that oxygen was often detected in spongy agglomerate. With a probe size of 10 nm for quantitative EDS analyses, every compositional result obtained is from a whole region including a few of nickel crystallites surrounded by BR. After leaching at 30–70 °C, aluminum in the catalyst is present mostly as alumina and/or alumina hydrates located on the surface [16, 25] or within the BR. Residue of alumina species in BR would, undoubtedly, result in an overestimated aluminum level of leaching products.

The leaching reaction proceeds rapidly. Devred et al. [16] showed that no significant compositional differences were detected for spongy agglomerate in the catalyst obtained by leaching of a Ni–50wt%Al alloy at 80 °C for 10 s to 2 h. Significant compositional differences were detected for the catalysts, which were prepared from different source Ni–50wt%Al alloys, i.e., more aluminum was

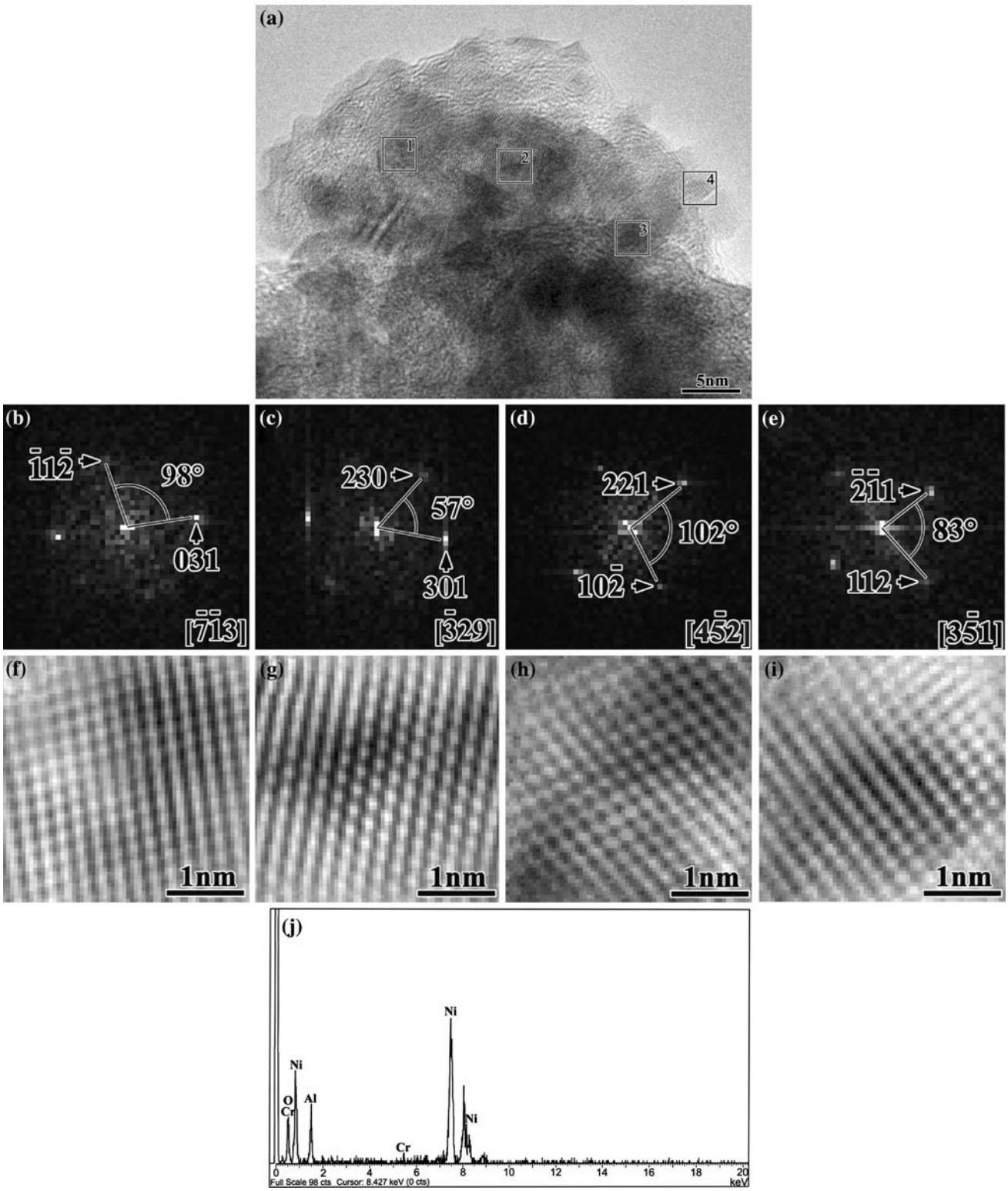

Fig. 3 (**a**) HRTEM image of the spongy agglomerate in the catalyst prepared by leaching at 70 °C for 90 min; (**b**–**e**) the diffractograms and (**f**–**i**) the Fourier-filtered images of the four crystal regions framed in (**a**), the zone axes are in turn $[\bar{7}\bar{1}3]$, $[\bar{3}29]$, $[4\bar{5}2]$ and $[3\bar{5}1]$ of oP16-Ni; (**j**) the EDS spectrum taken from one of the imaging regions

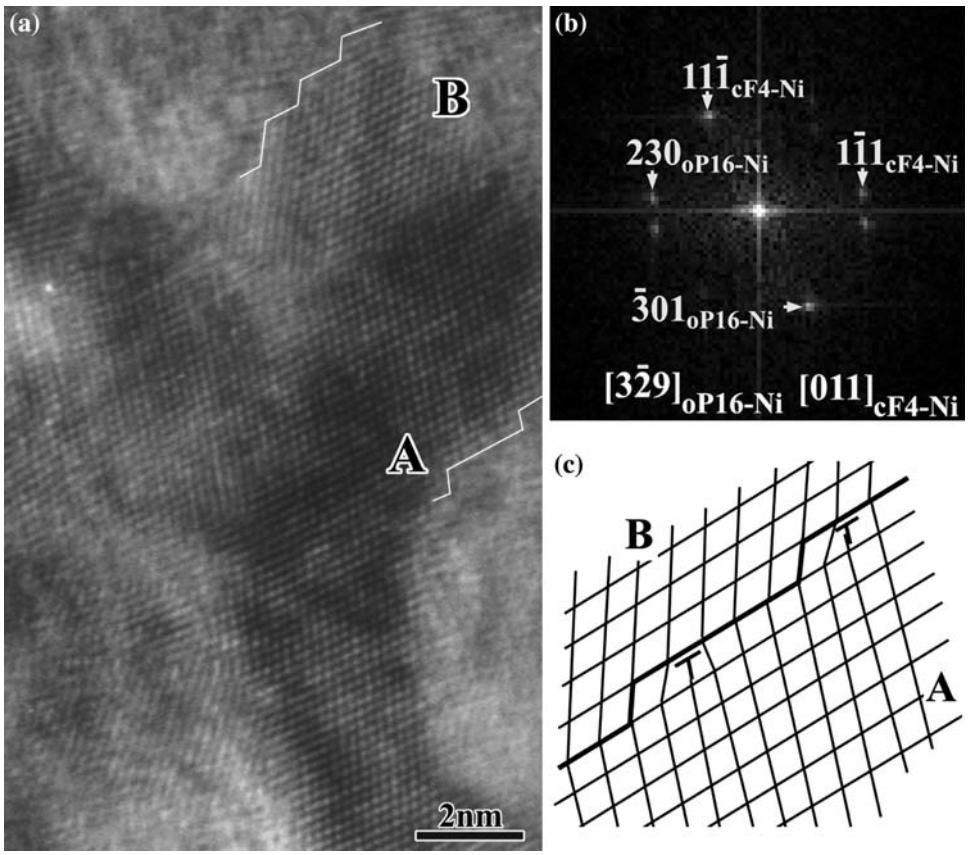

Fig. 4 (**a**) HRTEM image of the catalyst prepared by leaching at 30 °C for 20 min; (**b**) the diffractogram of the area including the regions, "A" and "B" marked in (**a**), the zone axis for the region "A" is [011] of cF4-Ni, and that for the region "B" is $[3\bar{2}9]$ of oP16-Ni; (**c**) an illustration of single-atomic steps and interfacial dislocations on a semicoherent boundary between the "A" and "B" regions

removed from the alloy with more $NiAl_3$ [16]. In this study, under various leaching conditions, the composition of leaching products was similar, close to those reported in previous works [16, 19]. We believe that the aluminum contents in both oP16-Ni and cF4-Ni are in a same level.

The leaching product, oP16-Ni, would be finally transformed into the stable cF4-Ni phase. Actually, evidence on such a transformation has been provided in a number of previous works, where for a pure $NiAl_3$ phase [15, 18, 19, 26] and Ni–50wt%Al alloys [13, 18] leaching at 90–107 °C in a 20–25% alkali solution leads to a complete transformation from source phases into the final product, cF4-Ni.

Based on our observations, we propose mechanisms for the structural transitions from the source phase, oP16-$NiAl_3$, to oP16-Ni and finally to cF4-Ni. Under the eroding effects of an alkaline solution, aluminum atoms in $NiAl_3$ are extracted out rapidly. The vacancies generated at the original aluminum sites of $NiAl_3$ appear to be filled immediately by the nearest nickel atoms to maintain the atomic arrangement of oP16-$NiAl_3$. Rapid reconstruction of residual atoms in the eroded regions generates spongy agglomerate within an original $NiAl_3$ grain.

The transition from oP16-Ni into cF4-Ni is proposed to be a polymorphic transformation through a diffusionless, nucleation-and-growth process. Generally speaking, if the leaching temperature is not sufficiently high (e.g., 70 °C used in this study), the transformation from oP16-Ni into cF4-Ni could proceed for a long period of time (e.g., more than 90 min).

Effects of the coexistence of oP16-Ni and cF4-Ni phases on the performance of Raney-Ni catalyst

In this study, we revealed that two types of nano-scale nickel crystallites, oP16-Ni and cF4-Ni, coexist in a Raney-Ni catalyst. The surrounding BR forms a microporous network with a pore size of 2–10 nm. The nano-scale characteristic of the microstructure ensures a large surface area and abundant active centers to the catalyst. On the other hand, on the wall of micropores the sub-nanometer scale crystalline facets (Fig. 4a) exhibit different atomic configurations. For instance, a local pseudo five-fold symmetry appears on the $(\bar{3}01)$ plane of oP16-Ni, as shown in Fig. 6, while a hexagonal symmetry on the {111} plane of cF4-Ni. The nickel atoms on these facets offer adsorbing sites preferentially for reactant molecules which have matching configurations to these sites [27]. We propose that the coexistence of the oP16-Ni and cF4-Ni phases provides Raney-Ni catalysts with heterogeneous active centers. The proposal is supported by a H_2 thermal programmed desorption (TPD) examination of Raney-Ni [28]. On the TPD profile presented two peaks with similar

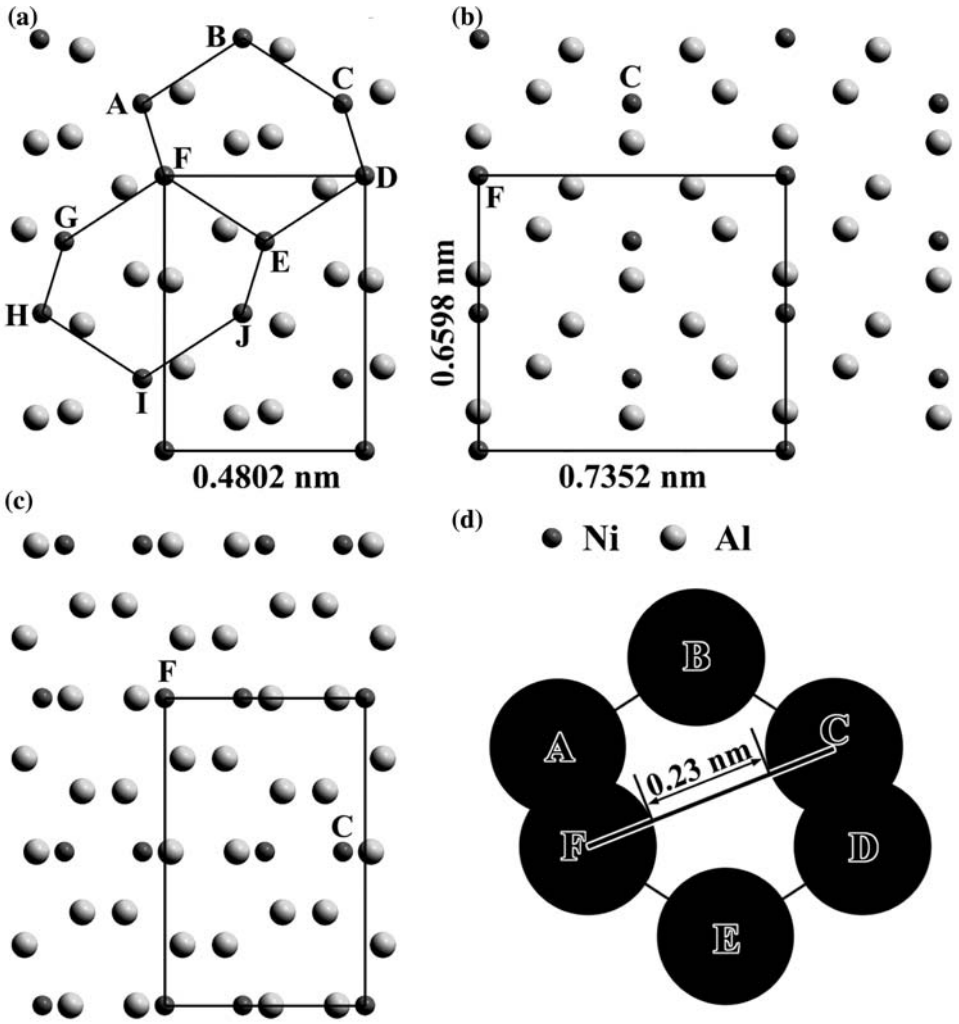

Fig. 5 Structure projections of oP16-$NiAl_3$ along (**a**) [010], (**b**) [001], and (**c**) [100] axis, the rectangle on every projection indicates a unit cell; (**d**) an illustration showing the crosswise width of the prism passage along the [010] direction

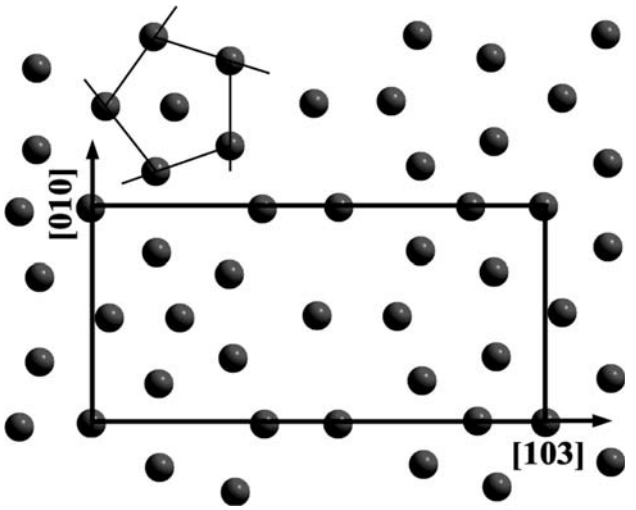

Fig. 6 Atomic arrangement on the $(\bar{3}01)$ plane of oP16-Ni showing a locally pseudo five-fold symmetry

intensities appearing at the temperature of 400 and 507 K, which correspond to loosely and strongly bound hydrogen species respectively. Our results suggest that for a specific hydrogenation reaction an optimal combination of oP16-Ni and cF4-Ni phases in a Raney-Ni catalyst could ensure high activity and selectivity. The volume ratio of these two active phases can be modified by either adjusting the composition and preparation methods of the starting alloy or altering the preparation conditions of the catalyst.

Conclusion

Leaching behaviors and structural transitions during aluminum leaching of the $NiAl_3$ phase in a 48.7wt% Ni–49.5wt%Al–1.0wt%Fe–0.8wt%Cr alloy is studied by X-ray diffraction, TEM, HRTEM together with EDS analyses. It is revealed that at the initial stage of leaching, $NiAl_3$ are fragmented into nano-scale grains. Based on the crystal structure of oP16-$NiAl_3$, a possible mechanism of grain fragmentation of the source phase is proposed. One type of nano-scale nickel crystallites, which preserves the atomic location of oP16-$NiAl_3$, is generated directly from the source phase. The newly discovered active phase,

oP16-Ni, coexists with cF4-Ni, a known active phase, in the Raney-Ni catalyst prepared by leaching at 30–70 °C, for 20–90 min in a 20 wt% sodium hydroxide solution and is further transformed into the stable cF4-Ni phase. The coexistence of the active phases, oP16-Ni and cF4-Ni, may enhance the performance of Raney-Ni.

Acknowledgements This study is supported partially by funding from the Chinese Institute of Petroleum Processing Research. We thank Dr. Baoning Zong for providing experimental materials for this study and Professors Enze Min, Wanzhen Lu and Drs. Baoning Zong, Xuhong Mu for fruitful and enlightening discussions.

References

1. Raney M (1925) US Patent 1,563,787
2. Raney M (1927) US Patent 1,628,191
3. Fasman AB, Mikhailenko SD, Maksimova NA, Ikhsanov ZhA (1983) Appl Catal 6:1. doi:10.1016/0166-9834(83)80182-1
4. Fouilloux P (1983) Appl Catal 8:1. doi:10.1016/0166-9834(83)80051-7
5. Hu H, Xie F, Pei Y, Qiao M, Yan S, He H et al (2006) J Catal 237:143. doi:10.1016/j.jcat.2005.11.001
6. Freel J, Pieters WJM, Anderson RB (1970) J Catal 16:281. doi:10.1016/0021-9517(70)90224-1
7. Kordulis C, Doumain B, Daman JP, Masson J, Dallons JL, Delannay F (1985) Bull Soc Chim Belg 1:371
8. Freel J, Pieters WJM, Anderson RB (1969) J Catal 14:247. doi:10.1016/0021-9517(69)90432-1
9. Lieber E, Morritz FL (1953) Adv Catal 5:417. doi:10.1016/S0360-0564(08)60647-1
10. Gros J, Hamar-Thibault S, Joud JC (1988) Surf Interface Anal 11:611. doi:10.1002/sia.740111206
11. Delannay F (1986) React Solids 2:235. doi:10.1016/0168-7336(86)80086-9
12. Hamar-Thibault S, Thibault J, Joud JC (1992) Z Metallk 83:258
13. Wang R, Lu Z, Ko T (2001) J Mater Sci 36:5645
14. Bakker ML, Young DJ, Wainwright MS (1988) J Mater Sci 23:3921. doi:10.1007/BF01106814
15. Colin P, Hamar-Thibault S, Joud JC (1992) J Mater Sci 27:2326. doi:10.1007/BF01105039
16. Devred F, Hoffer BW, Sloof WG, Kooyman PJ, van Langeveld AD, Zandbergen HW (2003) Appl Catal A 244:291. doi:10.1016/S0926-860X(02)00601-4
17. Lu Z, Wang R, Ko T, Chen H, Mu X, Zong B (1997) Chin J Catal 18:110
18. Sane S, Bonnier JM, Damon JP, Masson J (1984) Appl Catal 9:69. doi:10.1016/0166-9834(84)80039-1
19. Khaidar M, Allibert C, Driole J, Germi P (1982) Mater Res Bull 17:329. doi:10.1016/0025-5408(82)90081-2
20. Hamar-Thibault S, Koscielski T, Damon JP, Masson J (1989) J Catal 56:57
21. Pearson WB (1972) The crystal chemistry and physics of metals and alloys. Wiley-Interscience, New York, p 14
22. Bradley AJ, Taylor A (1937) Proc Roy Soc (Lond) A 159:56
23. Bradley AJ, Taylor A (1937) Philos Mag 23:1049
24. Chen H, Wang R (2008) Nucl Instrum Methods B 266:1062. doi:10.1016/j.nimb.2008.02.030
25. Robertson SD, Freel J, Anderson RB (1972) J Catal 24:130. doi:10.1016/0021-9517(72)90017-6
26. Sassoulas R, Trambouze Y (1964) Bull Soc Chim Fr 5:985
27. Balandin AA (1958) Adv Catal 10:96. doi:10.1016/S0360-0564(08)60405-8
28. Hu H, Qiao M, Wang S, Fan K, Li H, Zong B et al (2004) J Catal 221:612. doi:10.1016/j.jcat.2003.09.027